Modeling and Balance Control of SuperArm for Overhead Tasks

Jianwen Luo, Yao Su, Zelin Gong, Lecheng Ruan, Ye Zhao, H.Harry Asada, Chenglong Fu

***Abstract*—Overhead manipulation often needs collaboration of two operators, which is challenging in confined space such as in a compartment or on a ladder. Supernumerary Robotic Arm (SuperArm), as a promising wearable robotics solution for overhead tasks, can provide optimal assistance in terms of broader workspace, diverse manipulation functionalities, and labor-saving operations. However, the human-centered SuperArm interaction mechanism, taking into account human safety, is rarely studied to date, in particular, in the context of human standing balance. Motivated by this missing mechanism, our study proposes a novel method for the human-centered overhead tasks so that an individual operator can accomplish the overhead tasks with the assistance of SuperArm via tunable interaction force and support force regulation. The SuperArm-human interaction is modeled and a dynamics control method based on QR decomposition is adopted to decouple joint torques of the SuperArm and the interaction forces. As such, the supporting force can be regulated independently to guarantee the operator-SuperArm interaction forces in a safe region. Force plate is used for measuring the CoP position as an evaluation method of the standing balance. The critical horizontal push force is learned through experiment and used to guide the SuperArm balancing control. This method is implemented on a SuperArm prototype worn on the operator's back, providing necessary supporting forces for the overhead object while allowing the operator to move freely in the meantime.**

***Index Terms*—SuperArm, balance, overhead tasks, wearable robotics**

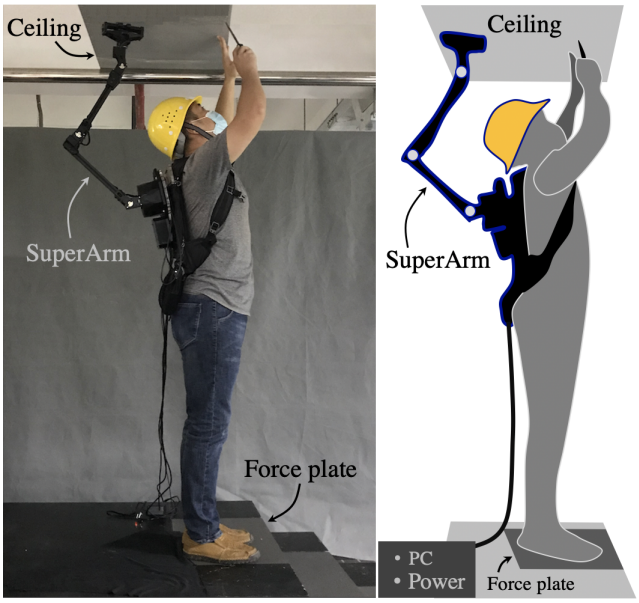

Fig. 1. A single operator is manipulating on the overhead ceiling with the SuperArm assisting in supporting it. Visual odometry device and F/T sensor are mounted on SuperArm for estimating the pose of the float base of SuperArm and the interaction force between operator and SuperArm.

I. Introduction

SUPERARM, as a pivotal branch of the SuperLimb family, is capable of assisting overhead tasks, especially those in a limited and narrow workspace. These tasks include a series of operations involving intensive workload and flexibility requirements in industrial set-ups, such as the compartment in aircraft [1]–[4]. The working space limitation impedes the entry of large-size robots or coexisted multi-operator collaboration. As an extension to exoskeletons and prostheses [5]–[7], SuperArm has the merit of extending the operator's workspace, augmenting human strength and allowing diverse postures beyond the human limb movement.

Among SuperLimb applications, overhead task assistance is able to provide additional supporting hands. In [8] a wearable robot secured on the shoulder is designed for assisting its wearer in the execution of tasks in the overhead workspace. Demonstration-based control using human demonstration data allows the robot to take a proactive and preemptive action as well as to confirm a successful transition. [4] explored a method to allow the operator to move freely while keeping a constant supporting force between the SuperLimb and the ceiling. Admittance control strategy is proposed to map the errors between the desired and the measured supporting force to the desired joint velocity. Although this work adopted an admittance control strategy to enable SuperArm to hold the object while the operator moves freely in space, it is yet an open question on how to regulate the supporting force while maintaining the safety of operator-SuperArm interaction force at the same time. This is an essential topic for human-centered wearable robotics. Compared to admittance controlled systems, utilizing the torque-based interaction mechanism in fully dynamics model allows compliant interaction with the environment and humans residing in the workspace of the

This work was supported in part by National Natural Science Foundation of China under Grant 51905251, China Postdoctoral Science Foundation under Grant 2019M662189, and Centers for Mechanical Engineering Research and Education at MIT and SUSTech. *(Corresponding author: C. Fu. Email: fucl@sustech.edu.cn)*

J. Luo, Z. Gong and C. Fu are with the Department of Mechanical Engineering, Southern University of Science and Technology, China. They are also with Centers for Mechanical Engineering Research and Education at MIT and SUSTech. J. Luo is also with School of Information Science and Technology, University of Science and Technology of China.

Y. Su and L. Ruan are with the Department of Mechanical and Aerospace Engineering, University of California, Los Angeles, USA.

Y. Zhao is with the George W. Woodruff School of Mechanical Engineering, Georgia Institute of Technology, USA.

H. H. Asada is with the Department of Mechanical Engineering, Massachusetts Institute of Technology, USA. He is also with Centers for Mechanical Engineering Research and Education at MIT and SUSTech.

robot [9], [10].

When the supporting force is larger than a certain threshold, the interaction force, especially the horizontal force, will degrade the stance balance. To address this problem, this study proposes a dynamics control based on the modeling of human-SuperArm interaction. This method is able to regulate the interaction and supporting forces. We define a stability criterion using center-of-pressure (CoP) and use it to evaluate the performance of the proposed method. The SuperArm works in the task space where the human body is braced through a coupling impedance. QR decomposition is adopted to decouple the dynamics model of SuperArm and human such that the supporting forces of the overhead task and joint torques are able to be controlled independently. A SuperArm prototype convenient to wear is built for experimental validation. Within our best knowledge, it is the first time to study the standing balance issue of SuperArm in the overhead task. The contributions of this letter lie in the following twofold:

(i) A SuperArm-human model which decouples joint torques of SuperArm and SuperArm-human interaction forces is established;

(ii) A balance controller based on the established model is proposed to regulate the interaction forces. CoP is chosen as an evaluation index for balance.

The rest of the letter is organized as follows. We review related work in Section II, and presents the modeling of SuperArm and human in Section III. Section IV proposes the balance control method based on the model of Section III. Section V demonstrates the experiment results. This line of research is concluded in Section VI.

II. Related Work

SuperLimb is an emerging field where some researchers explored applications in augmenting, assisting and restoring human functions and attracts accumulating attentions during recent years. To augment human capability, a SuperLimb prototype that assists an operator in holding objects, lifting weights, etc, is designed [11]. In [12] a wearable robot named supernumerary robotic limb is designed to assist human workers with additional arms and legs attached to the wearer's body for holding an object, positioning a workpiece, operating a powered tool, securing the human body, and more. [13] constructs a supernumerary robotic limb attached to the human waist to support the body efficiently when the human is taking fatiguing. In [14] a new type of wearable robot is introduced with two additional legs to balance assistance and joint load reduction for human bipedal walking is demonstrated. [15] presents a new type of supernumerary robotic limbs that supports the human body against floors, walls, and surrounding structures so that the human can perform a task safely, comfortably, and stably. For near-ground work, [16] designs a SuperLimb with impedance control to stably support the wearer's body. [17] demonstrates a new robotic human augmentation system that will assist the operator in carrying a heavy payload, reaching and maintaining difficult postures, and ultimately better performing their job. In [18] a wearable robotic forearm is demonstrated to enlarge the personal workspace for versatile tasks. In [19] a wearable robot named MantisBot Alpha is designed that braces a worker near the ground with two expandable robotic arms to perform bi-manual tasks and assist operator in standing up and kneeling down. In [20] a supernumerary leg powered by magnetorheological actuators is designed to assist walking. In [21] a method is presented to quantify the the usable degrees of freedom (DOFs) of a human body for a specific task so that the number of SuperLimb actuators can be reduced. [22] creates an explorative design of an ambient SuperLimb system that involves a pneumatically-driven robotic cane for at-home motion assistance, an inflatable vest for compliant human-robot interaction, and a depth sensor for ambient intention detection. In [23] a passive quadrupedal system consisting of a robotic augmentation named Extra Robotic Legs with two articulated robot legs and human operator is designed, which helps bear a heavy backpack payload.

In those works, researchers conduct inspiring explorations mainly in assisting and augmentation. With the equipment of SuperLimb, human's capability of handling versatile tasks is greatly leveraged. As another critical aspect, this letter mainly focuses on the balance in the overhead tasks.

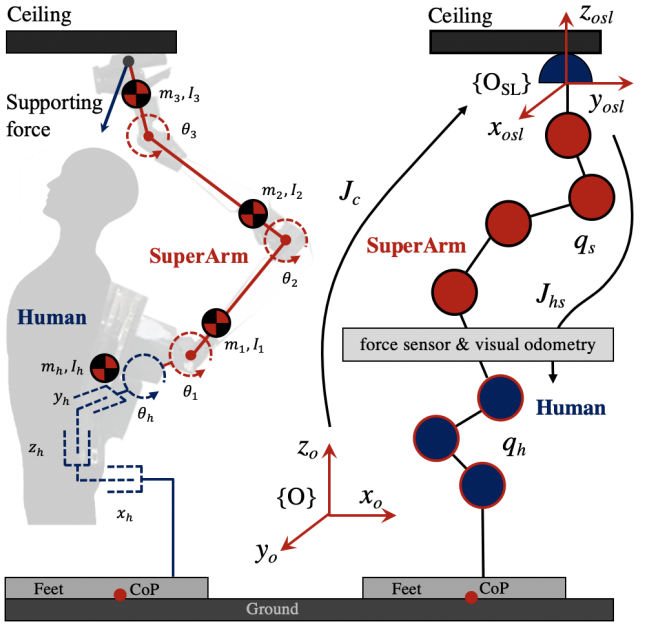

Fig. 2. The general model of SuperArm and operator. In this model, the operator is modeled as part of a manipulator, however, the joint positions and torques of the operator are not controllable.

III. Modeling of SuperArm

The SuperArm configuration is shown in Fig. 1, with its base fixed on the back of the operator via a shoulder belt. The total weight of our SuperArm prototype is 5 kg with joint-level torque control capability. The SuperArm on the operator is inherently modeled as a manipulator with a floating base. A visual odometry device mounted on the base of SuperArm measures the pose of the float base, and a F/T sensor mounted between SuperArm and operator measures the interaction force.

Our objective is to design a automatic control mechanism in which the SuperArm is able to guarantee human balance, provide sufficient supporting force, and regulate the interaction force between the operator and SuperArm to maintain human body stability. This mechanism considers the operator and SuperArm dynamics and computes desired SuperArm torque inputs based on the operator, SuperArm and environment states. These states are coupled in the dynamic model, and a null space-projection method based on QR decomposition [24] is employed to achieve multi-task decoupling.

A full dynamic model is developed to include the states from operator, SuperArm and the environment. Operator states include interaction forces between the operator and SuperArm, linear and rotational accelerations, linear and rotational velocities. The SuperArm states include joint position, velocity and torque. Environment states include the supporting force from SuperArm. The states and inputs of operator and SuperArm is integrated in this model to take into account the coupled human-SuperArm loop.

In this section, we will introduce the model in two levels: kinematics and dynamics models. In the kinematics model, the coupling of operator and SuperArm movement is analyzed in two different cases, and their motion relationship is given. In the dynamics model, an analytical solution for SuperArm torques is given to track certain movement of human body and the derivation of related supporting force is also provided.

A. Kinematics Model

The kinematics model studies the coupling of operator and SuperArm motion. Here $q_h \in \Re^{h\times 1}$ and $\tau_h \in \Re^{h\times 1}$ represent human joint position and torque states, respectively; $q_s \in \Re^{s\times 1}$ and $\tau_s \in \Re^{s\times 1}$ represent SuperArm joint position and torque states, respectively; s and h are the number of DoFs of SuperArm and human, respectively. Note that, τ_h is treated as a state in this model rather than an input. Our objective is to track q_h and regulate τ_h through control of the SuperArm. Our model only considers the condition $s > h$ since in general manipulator has more DoFs than that of human body to provide the capacity of accomplishing multi-tasks simultaneously. As shown in the frame O_{SL} of Fig. 2, q_h depends on q_s and components of q_h. Therefore, q_s and q_h obey:

$$q_h = f(q_{h2}, q_s), \tag{1}$$

where $q_h = [q_{h1}, q_{h2}]^T$ and q_{h2} are coupled states. A closed-kinematic chain exists in the model of Fig. 2, which also imposes an algebraic constraint. In this study, the kinematic model is categorized into two cases: 1) $s = h$ and 2) $s > h$.

Case 1 ($s = h$): in this cases q_h and q_s are decomposed into two components, $q_h = [q_{h1}, q_{h2}]^T$, $q_s = [q_{s1}, q_{s2}]^T$. We design q_{s2} to track q_{h2}, i.e. $q_{h2} = Kq_{s2}$, where K is selected as a constant coefficient matrix. If q_{h2} includes rotational DoFs, correspondingly q_{s2} is selected from rotation DoFs. Likewise, if q_{h2} includes translation DoFs, correspondingly q_{s2} is selected from translation DoFs. We can select K to cancel q_{h2} in (1) so that (1) can be simplified to $q_{h1} = f(q_{s1})$. Therefore, the derivative of that equation has,

$$\dot{q}_{h1} = \hat{J}_{hs}\dot{q}_{s1}, \tag{2}$$

where $\hat{J}_{hs}$ is the Jacobian with respect to frame O_{SL} as shown in Fig. 2. Combined with $q_{h2} = Kq_{s2}$, we have a relationship between q_h and q_s depicted as:

$$\dot{q}_h = J_{hs}\dot{q}_s = \begin{bmatrix} \hat{J}_{hs} & O \\ O & K \end{bmatrix} \dot{q}_s, \tag{3}$$

where J_{hs} and $\hat{J}_{hs}$ are square and invertible except at singularity, which is out of scope of this study. This singularity rarely occurs in our implementation. In that case, it makes sense to claim that the singularity does not matter a lot for this letter. From (3), $\dot{q}_s^d$ and q_s^d can be computed as:

$$\begin{cases} \dot{q}_s^d = J_{hs}^{-1}\dot{q}_h, \\ q_s^d - q_s^a = \Delta q_s = J_{hs}^{-1}\dot{q}_h, \end{cases} \tag{4}$$

where q_s^d and q_s^a are the desired and actual states respectively.

Case 2 ($s > h$): in the same way as case 1, we still decompose q_s and q_h into $[q_{s1}, q_{s2}]^T$ and $[q_{h1}, q_{h2}]^T$. And q_{h2} is set to be equal to $q_{h2} = Kq_{s2}$ with K being a constant coefficient matrix. We have the similar form:

$$\dot{q}_h = J_{hs}\dot{q}_s = \begin{bmatrix} \hat{J}_{hs} & O \\ O & K \end{bmatrix} \dot{q}_s, \tag{5}$$

where $\hat{J}_{hs} \in \Re^{h1\times s1}$ and $h_1 < s_1$. With svd-based pseudo inverse, we have the inverse of J_{hs} as:

$$\dot{q}_s = J_{hs}^{+}\dot{q}_h = \begin{bmatrix} \hat{J}_{hs}^{+} & O \\ O & K^{-1} \end{bmatrix} \dot{q}_h. \tag{6}$$

Thus $\dot{q}_s^d$ and q_s^d are computed in the same way as case 1:

$$\begin{cases} \dot{q}_s^d = J_{hs}^{+}\dot{q}_h, \\ q_s^d - q_s^a = \Delta q_s = J_{hs}^{+}\dot{q}_h. \end{cases} \tag{7}$$

In this design, SuperArm can spare some DoFs to compensate for the operator's posture. In the simplest way, SuperArm is designed such that all types of DoFs (translational and rotational) correspond to the motion DoFs of operator. However, translational DoFs usually spare large space and most manipulator configuration only includes rotational DoFs. Therefore, it is necessary to discuss the above method.

In this kinematics model, motion relationship between the operator and SuperArm is discussed with two cases considered. The decoupling method is adopted for SuperArm to track the operator motion.

B. Dynamics Model

A dynamical system is normally formulated as $\dot{x} = f(x, u)$, where x is the system states and u is the input. In this study, the dynamics with human in the loop is considered and interaction forces between operator and SuperArm as well as the operator's motion states are taken into account. The dynamics is formulated as:

$$\dot{x} = f(x, u_s, u_h), \tag{8}$$

where u_s and u_h are input of SuperArm and human respectively. $x = [x_s, x_h]^T$ is the system states, including SuperArm sates x_s and human states x_h respectively. Operator is modeled as a part of manipulator and includes 3 rotation DoFs and 3 translation DoFs as shown in Fig. 2. The complete dynamics equation is as:

$$A\ddot{q} + h = \tau + J_c^T \lambda, \tag{9}$$

where A is inertia matrix, h includes Coriolis force and gravity. τ is the joint torques of SuperArm and operator. λ is the supporting force. $J_c \in \Re^{k\times n}$ is the Jacobian of support point with respect to global frame O as shown in Fig. 2. k is the number of DoFs of contact constraint. Since it is assumed that the operator is equivalent to a manipulator with 6 DoFs, of which 3 DoFs are rotational and 3 DoFs are translational, q and τ are defined as:

$$\begin{cases} q = [q_s, q_h]^T, \\ \tau = [\tau_s, \tau_h]^T, \end{cases} \tag{10}$$

where the subscription s and h represent SuperArm and human respectively. $q_s \in \Re^{s\times 1}$ and $q_h \in \Re^{h\times 1}$. In this study, the condition in which $s \geq h$ is considered. Therefore, QR decomposition of J_c^T has the form as:

$$J_c^T = Q \begin{bmatrix} R \\ 0 \end{bmatrix}, \tag{11}$$

where Q is an orthogonal matrix and $Q^T Q = I$, $R \in \Re^{k\times k}$ is an upper triangular matrix with rank of k. Therefore, we have:

$$A\ddot{q} + h = \tau + Q \begin{bmatrix} R \\ 0 \end{bmatrix} \lambda. \tag{12}$$

The above equation is decomposed into two parts with λ extracted:

$$\begin{cases} S_k Q^T (A\ddot{q} + h - \tau) = R\lambda, \\ S_{kc} Q^T (A\ddot{q} + h) = S_{kc} Q^T \tau, \end{cases} \tag{13}$$

where the selection matrices S_k and S_{kc} are:

$$\begin{cases} S_k = [I_k, O_{k\times(n-k)}], \\ S_{kc} = [O_{(n-k)\times k}, I_{(n-k)\times(n-k)}]. \end{cases} \tag{14}$$

Therefore, the contact constrain is canceled from (14) and we have:

$$\begin{cases} \tau = (S_{kc} Q^T)^\dagger S_{kc} Q^T (A\ddot{q} + h), \\ \lambda = R^{-1} S_k Q^T N_{kc} (A\ddot{q} + h), \end{cases} \tag{15}$$

where $(\cdot)^\dagger$ is dynamically consistent pseudo-inverse [25], i.e. $W^\dagger = A^{-1}W^T(WA^{-1}W^T)^{-1}$. $N_{kc} = I - (S_{kc}Q^T)^\dagger S_{kc} Q^T$ is the null projection of $S_{kc}Q^T$. $\tau = [\tau_s, \tau_h]^T$, where τ_s is the joint torque of SuperArm and τ_h is the joint torque of human. $\ddot{q} = [\ddot{q}_s, \ddot{q}_h]^T$ includes the joint acceleration of SuperArm and human.

The task space above is defined in frame O_{SL} as shown in Fig. 2. The analytical solution given by (15) is only one of many feasible ones due to the pseudo inverse used. Therefore, the solution (15) is not unique. In this dynamic model, joint torques of SuperArm and human τ are decoupled with the contact force λ, which is the supporting force for overhead task. Using (15), we can compute the τ and λ using joint acceleration.

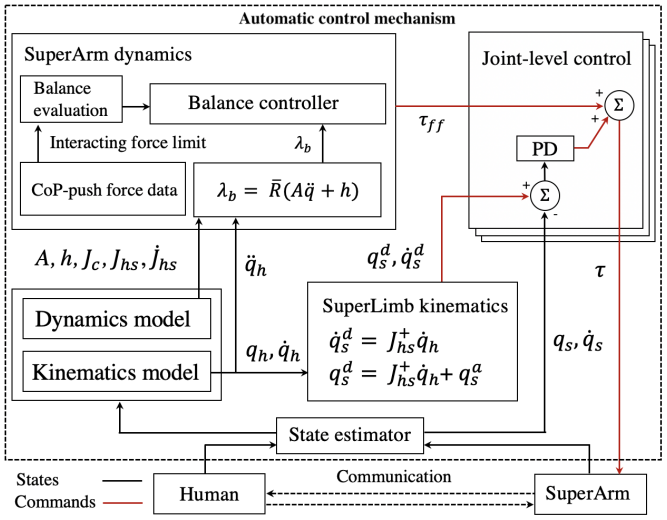

Fig. 3. Automatic control mechanism of proposed balance controller for overhead task. The detailed communication mechanism is demonstrated in the dashed box to show the workflow proposed in this letter. Red lines are commands and black lines are states.

This letter aims to regulate the interaction forces and contact forces, which corresponds to τ_h and λ. (15) is able to provide an efficient solution for joint torque and supporting force. However, this solution does not take human body stability into consideration. To ensure the CoP stability of the operator, a balance control problem is formulated in the next section.

IV. Balance Control

A. Full-body Dynamics Control

Section III demonstrates a solution to τ and λ using joint acceleration of SuperArm and human. Given a desired joint acceleration, a feasible τ and λ can be computed. The desired acceleration is :

$$\ddot{q}_s = J_{hs}^\dagger (\ddot{q}_h - \dot{J}_{hs}\dot{q}_s), \tag{16}$$

where $\ddot{q}_h$ is the actual acceleration of human and J_{hs} is the Jacobian from frame O_{hs} to q_h. Thus the desired acceleration $\ddot{q}^d = [\ddot{q}_s^d, \ddot{q}_h^d]^T$.

The solution for supporting force in (15) is the optimal result under kinetic energy as cost function. It is the force that compensates all gravity of SuperArm. We use λ_b as the basic force:

$$\lambda_b = \bar{R}(A\ddot{q} + h), \tag{17}$$

where λ_b is the force for supporting gravity of SuperArm itself. $\bar{R} = R^{-1} S_k Q^T N_{kc}$. $J_c^T \lambda_b$ is the joint torque for compensation of gravity and dynamics terms. If desired supporting force is λ_s, then the aggregated joint torque and corresponding supporting force is:

$$\begin{cases} \tau = J_c^T (\lambda_b - \lambda_s), \\ \lambda = \bar{R}(A\ddot{q} + h - \tau). \end{cases} \tag{18}$$

Algorithm 1 Balance Control Algorithm

Input: $q_h, \dot{q_h}, \ddot{q_h}, (\lambda_s, \bar{\tau}_h)$ constant

Output: $\tau_{regulate}$

Initialize: $S_k \Leftarrow [I_k, O_{k\times(n-k)}]$
$S_{kc} \Leftarrow [O_{(n-k)\times k}, I_{(n-k)\times(n-k)}]$
$\alpha \Leftarrow \beta^{-n}$
while $x_{CoP} > \bar{x}_{CoP}$ **do**
  $q_s \Leftarrow$ Kinematics model (q_h)
  $q \Leftarrow [q_s, q_h]^T$
  $A, h, J_c, J_{hs}, \dot{J}_{hs} \Leftarrow$ Dynamics model $(q, \dot{q})$
  $\dot{q}_s \Leftarrow J_{hs}^{-1}\dot{q}_h, \quad \ddot{q}_s \Leftarrow J_{hs}^{\dagger}(\ddot{q}_h - \dot{J}_{hs}\dot{q}_s)$
  $\dot{q} \Leftarrow [\dot{q}_s, \dot{q}_h]^T, \quad \ddot{q} \Leftarrow [\ddot{q}_s, \ddot{q}_h]^T$
  $Q, R \Leftarrow$ QR decomposition of J_c
  $Aqh \Leftarrow A\ddot{q} + h$
  $\tau_b \Leftarrow (S_{kc}Q^T)^{\dagger}S_{kc}Q^T Aqh$
  $\lambda_b \Leftarrow R^{-1}S_k Q^T N_{kc} Aqh$
  $\tau \Leftarrow Aqh - J_c^T(\lambda_b - \lambda_s), \quad \tau_h \Leftarrow [\tau(4), \tau(5)]^T$
  $Aqh_s \Leftarrow Aqh(1:2,:), \quad Aqh_h \Leftarrow Aqh(4:5,:)$
  $J_{cs} \Leftarrow J_c(1:2, 1:2), \quad J_{ch} \Leftarrow J_c(1:2, 4:5)$
  $W_1 \Leftarrow J_{cs}^T(J_{ch}^T)^{-1}, \quad W_2 \Leftarrow Aqh_s - J_{cs}^T(J_{ch}^T)^{-1}Aqh_h$
  $\tau_s^a \Leftarrow \alpha W_1(\bar{\tau}_h - \tau_h) + W_2$
  $\tau_s^d \Leftarrow PI(\tau_s^a)$
  $\lambda \Leftarrow (J_{cs}^T)^{-1}(Aqh_s - \tau_s^d)$
  $\tau_{regulate} \Leftarrow Aqh - J_c^T\lambda$
end while

In this section we formulate the balance control of human body as a torque regulation problem and propose a balance controller which is able to calculate the desired torque inputs for SuperArm to regulate the interaction force between the operator and SuperArm. And combining with the basic solution we derived in Section III, this whole automatic control mechanism is shown in Fig 3.

To better investigate the relationship of τ_s and τ_h, and design a controller for τ_s to track the desired interaction torque $\bar{\tau}_h$, we can rewrite (18) into the following form.

$$\begin{bmatrix} Aqh_s \\ Aqh_h \end{bmatrix} = \begin{bmatrix} \tau_s \\ \tau_h \end{bmatrix} + \begin{bmatrix} J_{cs}^T \\ J_{ch}^T \end{bmatrix} \lambda, \tag{19}$$

where $Aqh = A\ddot{q} + h$, Aqh_s is the first two rows of Aqh, Aqh_h is the 4th and 5th row of Aqh, $J_{cs} = J_c(1:2, 1:2)$ and $J_{ch} = J_c(1:2, 4:5) \in \Re^{2\times 2}$. $\tau_h = [\tau_{hx}, \tau_{hy}]^T$ is the interaction forces including the horizontal force τ_{hx} and τ_{hy}. The above equation is able to be decoupled as below:

$$\begin{cases} \lambda = (J_{cs}^T)^{-1}(Aqh_s - \tau_s), \\ \lambda = (J_{ch}^T)^{-1}(Aqh_h - \tau_h). \end{cases} \tag{20}$$

Within the scope of this study, the singularity of J_{cs} and J_{ch} is not considered, which never exists in the current configuration of the human and SuperArm. Therefore, J_{cs} and J_{ch} are always taken as invertible. Therefore, we have:

$$\tau_s = W_1\tau_h + W_2, \tag{21}$$

where $W_1 = J_{cs}^T(J_{ch}^T)^{-1}$ and $W_2 = Aqh_s - J_{cs}^T(J_{ch}^T)^{-1}Aqh_h$.

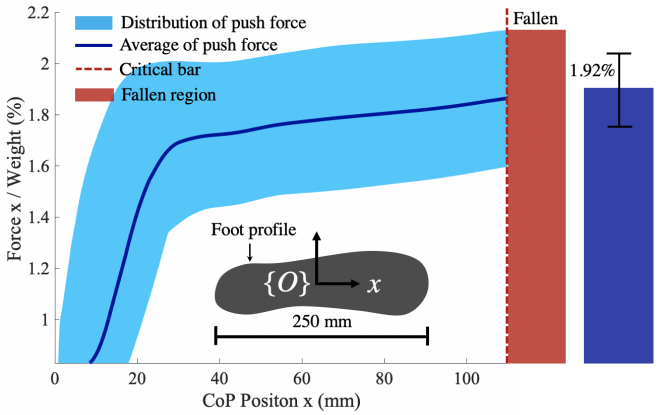

Fig. 4. Push force versus CoP position within the supporting feet in anterior-posterior direction. Blue line the average push force trajectory and blue region is the distribution of push force. Human starts to fall when CoP moves beyond 110 mm within the frame of O. The average ratio of critical push force and subject and SuperArm's total weight is 1.92 %.

(21) represents the coupling relationship between interaction forces τ_h and SuperArm joint torques τ_s.

τ_s^a represents desired value of τ_s, and it is designed as below:

$$\tau_s^a = \alpha W_1(\bar{\tau}_h - \tau_h) + W_2, \tag{22}$$

where $\bar{\tau}_h$ is the desired interaction force. α is named as the convergence coefficients and set as below:

$$\alpha = \beta^{-n}. \tag{23}$$

A PI controller is adopted to track τ_s^a. And the PI control law is as below:

$$\tau_s^d = K_p e + K_i \int_0^t e\delta t, \tag{24}$$

where $e = \tau_s^d - \tau_s^a$. After plugging back τ_s^d into (20) and combining with (18) we can have the expression of regulated torque command $\tau_{regulate}$, which is the feed forward signal for SuperArm joints to track.

$$\tau_{regulate} = Aqh - J_c^T\lambda. \tag{25}$$

In this subsection, a balance control based on the dynamics model of human-SuperArm is proposed. Human is modeled as the part of the manipulation where the DoFs of human movement is uncontrollable. DoFs of human and the DoFs of the SuperArm are coupled in the dynamics model. This study analyzed the relationship between the human movement and the SuperArm and proposed a balance controller aiming at attenuating the disturbance of the horizontal interaction force so as to keep human's standing balance.

The algorithm of the proposed controller is shown in Algorithm 1. x_{CoP} is the position of CoP within the foot coordinate. $\bar{x}_{CoP}$ is the safe threshold in which case human is able to keep standing balance.

B. Simulation

In this subsection, an example is demonstrated using the method proposed in the previous section. Due to the hardware condition in our study, a SuperLimb with three DoFs is worn

on the operator. Human moves in $x_0 - z_0$ plane as shown in Fig. 2. In this case, human has three DoFs, i.e. x_h, y_h and θ_h. Supporting force $\lambda = [\lambda_x, \lambda_y]^T$.

In this example, $s = h = 3$, $q_s = [\theta_{s1}, \theta_{s2}, \theta_{s3}]^T$, $q_h = [x_h, y_h, \theta_h]^T$. We select $q_s = [q_{s1}, q_{s2}]^T$ where $q_{s1} = [x_h, y_h]^T$, $q_{s2} = \theta_h$. $q_h = [q_{h1}, q_{h2}]^T$ where $q_{h1} = [x_h, y_h]^T$ and $q_{h2} = \theta_h$. Based on the discussion in previous section, we set $\theta_h = \pi/4 - \theta_1$ to keep the posture of 1st SuperLimb link relatively static in the global frame.

$$\begin{bmatrix} \dot{x}_h \\ \dot{y}_h \\ \dot{\theta}_h \end{bmatrix} = \begin{bmatrix} l_2 s_{2c} + l_3 s_{23c} & l_3 s_{23c} & 0 \\ -l_2 c_{2c} - l_3 c_{23c} & -l_3 c_{23c} & 0 \\ 0 & 0 & -1 \end{bmatrix} \begin{bmatrix} \dot{\theta}_2 \\ \dot{\theta}_3 \\ \dot{\theta}_1 \end{bmatrix}, \quad (26)$$

where s_{xyc} stands for $sin(x + y + c)$ and c_{xyc} stands for $cos(x + y + c)$. $l_x, (x = 1, 2, 3)$ is the length of 1st, 2nd and 3rd SuperArm link. $l_x, (x = 11, 22, 33)$ is the position of 1st, 2nd and 3rd SuperArm link CoM. c is the constant angle and in this case $c = \pi/4$.

$$J_{hs} = \begin{bmatrix} l_2 s_{2c} + l_3 s_{23c} & l_3 s_{23c} & 0 \\ -l_2 c_{2c} - l_3 c_{23c} & -l_3 c_{23c} & 0 \\ 0 & 0 & -1 \end{bmatrix}. \quad (27)$$

The CoP data is measured when human stand statically. The subject is required to stand on a force plate which is able to measure the CoP position. Push force is exerted on the back where SuperArm's base is attached. The relationship between CoP's relative position within the supporting profile of the feet and the pushing force is visualized in Fig. 4. There appears a threshold for the safe pushing force where the pushing force lower than the threshold will be safe to the human standing balance. Base on the statistic result, a balance controller with CoP-related pushing force as performance evaluation is proposed.

In the simulation, the initial states of the SuperArm and the operator are in statically stable state and the operator stands without horizontal interaction force. When the operator's movement incurs the increasing of the horizontal interaction force, balance controller attenuates both the horizontal interaction force and vertical supporting force. For the overhead task, vertical supporting force is necessary while horizontal supporting force is not needed. However, horizontal supporting force is correlated to the horizontal interaction force which human stance balance is sensitive to. Fig. 5 and Fig. 6 show the evolution of the joint torques and the interaction forces when horizontal interaction force appears.

In Fig. 5, the first three rows show the joint torques and the fourth and fifth rows show the horizontal and vertical interaction forces respectively. The blue lines represent the forces that compensate the gravity of SuperArm. The red lines represents the forces when horizontal forces' disturbance appear. The black lines represent how the forces converge under the balance controller.

From τ_x and τ_y in Fig. 5 it is demonstrated that the horizontal and vertical interaction forces are able to be regulated independently. With the balance controller, the horizontal interaction force is attenuated and converge back to around zero force. Fig. 6 demonstrates that the supporting forces are decoupled. Horizontal supporting force converge back to

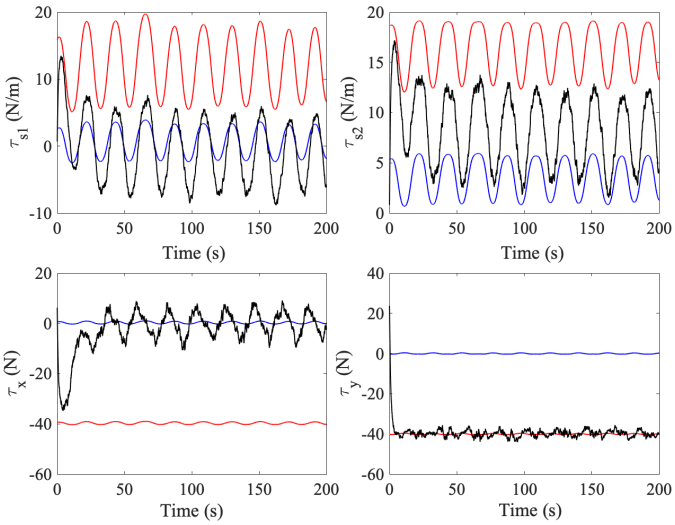

Fig. 5. Joint torques of SuperArm and interaction forces. τ_{s1} and τ_{s2} are the joint torques of SuperArm. τ_x and τ_y are the horizontal and vertical interaction forces. The blue lines are the basic forces to compensate the gravity of SuperArm itself. The red lines are the forces after disturbance. The black lines converge due to the balance control.

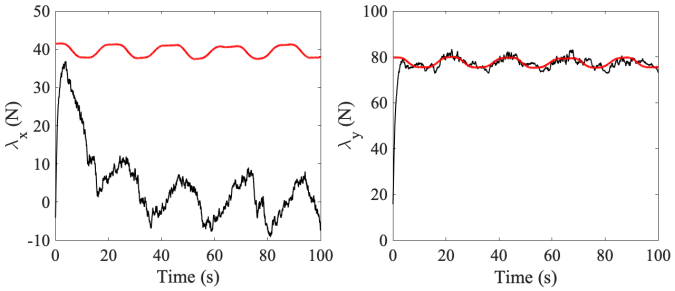

Fig. 6. Supporting forces converge due to the balance controller. The red lines are the supporting forces after disturbance. Black lines represents the convergence of the horizontal force under the balance controller.

around zero while vertical supporting force stays constant.

Fig. 7 show the tracking of τ_s where the red lines are τ_s^d and the blue lines are the tracking torques τ_s^a. The noises are added in the desired torque commands. Supporting forces are two dimensional and therefore in this case only two DoFs of SuperArm are needed to control the supporting forces. The first and second joints are selected which correspond to τ_{s1} and τ_{s2}. The model of SuperArm and human is nonlinear and consistent for overhead tasks. The balance controller is based

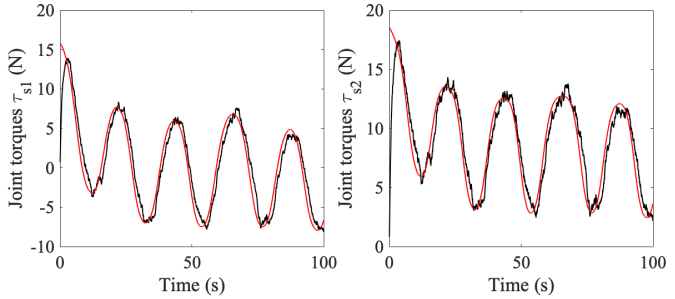

Fig. 7. The torque tracking of the SuperArm. The red lines are the desired torques and the black lines are the actual tracking torques.

on PI control which is stable and extensively verified in many theories and experiments.

V. Experiment

In this section, experiment is conducted to verify the balance controller proposed in this study. The operator's movement is constrained in Sagittal plane. The vertical movement does not affect the standing balance. Therefore, we focus on the horizontal movement in the experiment.

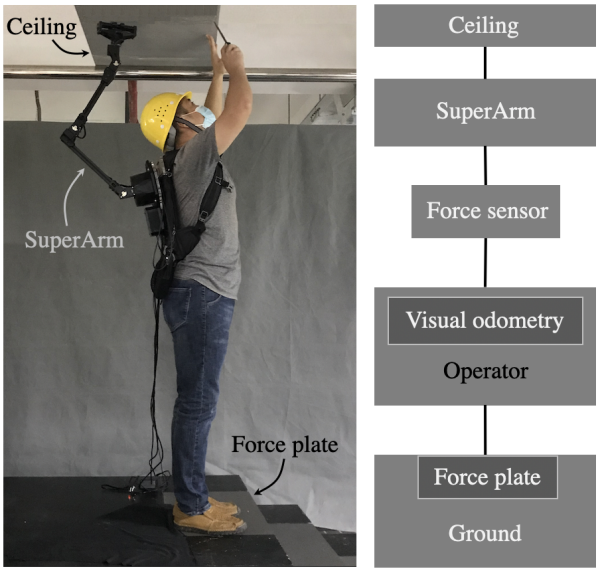

Fig. 8. The experiment scenario for overhead task. To evaluate the balance performance, subject stands on a force plate which is able to measure the CoP position.

A. Experiment Configuration

Fig. 8 demonstrates the experiment scenario. A off-the-shelf manipulator Interbotix VX300 was selected as the main mechanism. The manipulator weights around 4 kg which is suitable for a normal adult both in weight and size. There are five DoFs in total on VX300 manipulator while only three revolute joint in the Sagittal plane of the operator are adopted, which corresponds to θ_1, θ_2 and θ_3 in Fig. 2. A 6-axis force sensor is mounted between the base of VX300 manipulator and a rectangle-shaped acrylic board. The acrylic board is embedded in a backpack and tightly attached with the backpack. The force sensor is able to measure the interaction force between the operator and SuperArm. A visual odometry is mounted on the base of VX300 to measure the movement of the operator. Intel RealSense T265 is adopted as the visual odometry. A host PC with linux system runs the controller codes. ROS is adopted for running the controller of SuperArm and collecting the sensing data from the force sensor and the visual odometry. Interbotix manipulator is set as current mode so that the joints are torque-based control. The serial communication cable connects the SuperArm and the host PC. The force plate measures the CoP of the operator. The sample rates of the force sensor and visual odometry are 1kHz and 200Hz respectively. The data are synchronized during the experiment. It is noteworthy that the force plate is for evaluation purpose in the experiment rather than in the reality application due to the inconvenience of portability. Based on the results in Fig. 4, critical push force which incurs the fallen of human in stance state is statistically learned and normalized taking human weight into account.

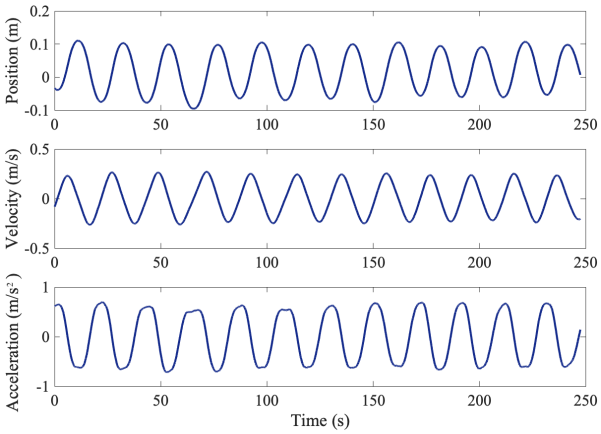

Fig. 9. The position, velocity and acceleration of human movement due to the disturbance in standing status.

B. Experiment Results

In experiment, the operator moves slightly in horizontal direction to induce unexpected disturbance forces. Balance controller regulates the SuperArm's joint torques to attenuate the horizontal interaction force to keep the operator's standing balance. Visual odometry measures the position, velocity and acceleration of the operator's main body and outputs position. Velocity and acceleration are differentiated from position once and twice respectively. Filter is also adopted to smooth the velocity and acceleration.

Fig. 9 shows the position, velocity and acceleration of the operator's movement. The movement is measured through the visual odometry mounted on the base of SuperArm.

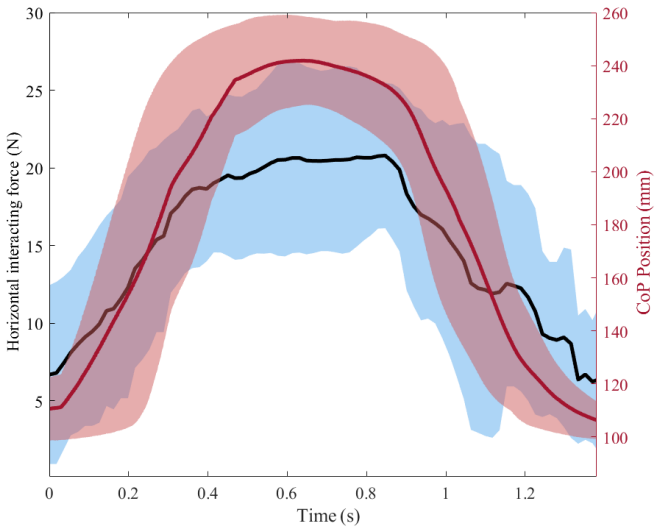

Fig. 10. Horizontal interaction force and CoP position. The black and red line are the horizontal interaction force and CoP position respectively. The lines are the statistical average results and the red and blue regions are the distributions of the experiment results.

Fig. 10 demonstrates the performance of balance controller. CoP position measured by force plate is used for perfor-

mance evaluation. At the beginning, the disturbing horizontal interaction force increases and push the CoP away from the center of supporting feet. Balance controller attenuates the horizontal interaction force through regulating the SuperArm's joint torques. When the horizontal interaction force converge back to around 5N and CoP position returns to the initial location where the operator stands in statically stable balance.

VI. Conclusion

This study proposed a model of a SuperArm and human for the overhead task and designed a balance control to avoid potential fallen danger. QR decomposition is used to decouple the supporting forces and the joint torques so as to control the interaction forces independently. The balance controller is able to attenuate the horizontal interaction force between the operator and the SuperArm so as to keep the standing balance. To quantify the evaluation of the balance, CoP position is used as the balance index. A SuperArm prototype is built on which force sensor and visual odometry are mounted to verify the effectiveness of the balance controller. Some conclusions include:

1) Standing balance is able to be guaranteed through regulating the joint torques of SuperArm;

2) The model of the SuperArm is able to present the internal properties;

3) The balance controller proposed in this letter is able to attenuate the horizontal interacting force which is potentially detrimental to the standing balance.

In experiment, balance controller is tested with force plate measuring the CoP position. Within our best knowledge, it is the first time to study the standing balance issue of SuperArm control for the overhead tasks. Usually the workspace of the operator is narrow and the operator is unable to separate two feet to enlarge the supporting region. Therefore, minimizing the horizontal interaction force to prevent falling is indispensable.

The controller proposed in this letter is related to the configuration of the SuperArm. Therefore, the future work will include the comprehensive discussion of the relationship between the controllability and the mechanical configuration of the SuperArm. A compact SuperArm with controller and electric power embedded will be designed.

References

[1] F. Parietti and H. H. Asada, "Supernumerary robotic limbs for aircraft fuselage assembly: body stabilization and guidance by bracing," in *2014 IEEE International Conference on Robotics and Automation (ICRA)*. IEEE, 2014, pp. 1176–1183.

[2] J. W. Guggenheim and H. H. Asada, "Inherent haptic feedback from supernumerary robotic limbs," *IEEE Transactions on Haptics*, pp. 1–1, 2020.

[3] J. Whitman and H. Choset, "Task-specific manipulator design and trajectory synthesis," *IEEE Robotics and Automation Letters*, vol. 4, no. 2, pp. 301–308, 2019.

[4] Z. Bright and H. H. Asada, "Supernumerary robotic limbs for human augmentation in overhead assembly tasks," in *Proc. Robot.: Sci. Syst.*, 2017, doi:10.15607/RSS.2017.XIII.062.

[5] K. Zhang, J. Luo, W. Xiao, W. Zhang, H. Liu, J. Zhu, Z. Lu, Y. Rong, C. W. de Silva, and C. Fu, "A subvision system for enhancing the environmental adaptability of the powered transfemoral prosthesis," *IEEE Transactions on Cybernetics*, pp. 1–13, 2020.

[6] M. Hao, J. Zhang, K. Chen, H. Asada, and C. Fu, "Supernumerary robotic limbs to assist human walking with load carriage," *Journal of Mechanisms and Robotics-Transactions of the ASME*, pp. 1–18, 2020.

[7] X. Yang, T. Huang, H. Hu, S. Yu, S. Zhang, X. Zhou, A. Carriero, G. Yue, and H. Su, "Spine-inspired continuum soft exoskeleton for stoop lifting assistance," *IEEE Robotics and Automation Letters*, vol. 4, no. 4, pp. 4547–4554, 2019.

[8] B. L. Bonilla and H. H. Asada, "A robot on the shoulder: Coordinated human-wearable robot control using coloured petri nets and partial least squares predictions," in *2014 IEEE International Conference on Robotics and Automation (ICRA)*, 2014, pp. 119–125.

[9] A. Dietrich, T. Wimbock, A. Albu-Schaffer, and G. Hirzinger, "Reactive whole-body control: Dynamic mobile manipulation using a large number of actuated degrees of freedom," *IEEE Robotics & Automation Magazine*, vol. 19, no. 2, pp. 20–33, 2012.

[10] J. Luo, Y. Zhao, D. Kim, O. Khatib, and L. Sentis, "Locomotion control of three dimensional passive-foot biped robot based on whole body operational space framework," in *2017 IEEE International Conference on Robotics and Biomimetics (ROBIO)*, 2017, pp. 1577–1582.

[11] B. Llorens-Bonilla, F. Parietti, and H. Asada, "Demonstration-based control of supernumerary robotic limbs. intelligent robots and systems (iros), 2012 ieee," in *RSJ International Conference on*, 2012, pp. 7–12.

[12] F. Parietti and H. H. Asada, "Dynamic analysis and state estimation for wearable robotic limbs subject to human-induced disturbances," in *2013 IEEE International Conference on Robotics and Automation*, 2013, pp. 3880–3887.

[13] F. Parietti, K. Chan, and H. H. Asada, "Bracing the human body with supernumerary robotic limbs for physical assistance and load reduction," in *2014 IEEE International Conference on Robotics and Automation (ICRA)*, 2014, pp. 141–148.

[14] F. Parietti, K. C. Chan, B. Hunter, and H. H. Asada, "Design and control of supernumerary robotic limbs for balance augmentation," in *2015 IEEE International Conference on Robotics and Automation (ICRA)*, 2015, pp. 5010–5017.

[15] F. Parietti and H. Asada, "Supernumerary robotic limbs for human body support," *IEEE Transactions on Robotics*, vol. 32, no. 2, pp. 301–311, 2016.

[16] D. A. Kurek and H. H. Asada, "The mantisbot: Design and impedance control of supernumerary robotic limbs for near-ground work," in *2017 IEEE International Conference on Robotics and Automation (ICRA)*, 2017, pp. 5942–5947.

[17] D. J. Gonzalez and H. H. Asada, "Design of extra robotic legs for augmenting human payload capabilities by exploiting singularity and torque redistribution," in *2018 IEEE/RSJ International Conference on Intelligent Robots and Systems (IROS)*, 2018, pp. 4348–4354.

[18] V. Vatsal and G. Hoffman, "Design and analysis of a wearable robotic forearm," in *2018 IEEE International Conference on Robotics and Automation (ICRA)*. IEEE, 2018, pp. 1–8.

[19] K. S. Hahm and H. H. Asada, "Design of a fail-safe wearable robot with novel extendable arms for ergonomic accommodation during floor work," in *2019 IEEE/RSJ International Conference on Intelligent Robots and Systems (IROS)*, 2019, pp. 8179–8184.

[20] C. Khazoom, P. Caillouette, A. Girard, and J. Plante, "A supernumerary robotic leg powered by magnetorheological actuators to assist human locomotion," *IEEE Robotics and Automation Letters*, vol. 5, no. 4, pp. 5143–5150, 2020.

[21] J. Guggenheim, R. Hoffman, H. Song, and H. H. Asada, "Leveraging the human operator in the design and control of supernumerary robotic limbs," *IEEE Robotics and Automation Letters*, vol. 5, no. 2, pp. 2177–2184, 2020.

[22] X. Wu, H. Liu, Z. Liu, M. Chen, F. Wan, C. Fu, H. Asada, Z. Wang, and C. Song, "Robotic cane as a soft superlimb for elderly sit-to-stand assistance*," in *2020 3rd IEEE International Conference on Soft Robotics (RoboSoft)*, 2020, pp. 599–606.

[23] D. J. Gonzalez and H. H. Asada, "Passive quadrupedal gait synchronization for extra robotic legs using a dynamically coupled double rimless wheel model," in *2020 IEEE International Conference on Robotics and Automation (ICRA)*, 2020, pp. 3451–3457.

[24] M. Mistry, J. Buchli, and S. Schaal, "Inverse dynamics control of floating base systems using orthogonal decomposition," in *2010 IEEE International Conference on Robotics and Automation*, 2010, pp. 3406–3412.

[25] L. Sentis and O. Khatib, "Control of free-floating humanoid robots through task prioritization," in *Proceedings of the 2005 IEEE International Conference on Robotics and Automation*, 2005, pp. 1718–1723.